

Comparison between Protein–Polyethylene Glycol (PEG) Interactions and the Effect of PEG on Protein–Protein Interactions Using the Liquid–Liquid Phase Transition

Ying Wang and Onofrio Annunziata*

Department of Chemistry, Texas Christian University, Fort Worth, Texas 76129

Received: August 29, 2006; In Final Form: November 18, 2006

Phase transitions of protein aqueous solutions are important for protein crystallization and biomaterials science in general. One source of thermodynamic complexity in protein solutions and their phase transitions is the required presence of additives such as polyethylene glycol (PEG). To investigate the effects of PEG on the thermodynamic behavior of protein solutions, we report measurements on the liquid–liquid phase separation (LLPS) of aqueous bovine serum albumin (BSA) in the presence of relatively small amounts of PEG with an average molecular weight of 1450 g/mol (PEG1450) as a model system. We experimentally characterize two thermodynamically independent properties of the phase boundary: (1) the effect of PEG1450 concentration on the LLPS temperature, (2) BSA/PEG1450 partitioning in the two liquid coexisting phases. We then use a thermodynamic perturbation theory to relate the first property to the effect of PEG concentration on protein–protein interactions and the second property to protein–PEG interactions. As criteria to determine the accuracy of a microscopic model, we examine the model's ability to describe both experimental thermodynamic properties. We believe that the parallel examination of these two properties is a valuable tool for verifying the validity of existing models and for developing more accurate ones. For our system, we have found that a depletion–interaction model satisfactorily explains both protein–PEG interactions and the effect of PEG concentration on protein–protein interactions. Finally, due to the general importance of LLPS, we will experimentally show that protein–PEG–buffer mixtures can exhibit two distinct types of liquid–liquid phase transitions.

Introduction

Understanding the mechanism of phase transformations of protein aqueous solutions is important for several applications in materials science and biotechnology. In protein crystallography, it is important for the production of protein crystals, the bottleneck to the determination of the molecular structure of a protein.^{1,2} In pharmaceutical science, it is important for the preparation of protein microspheres relevant to drug delivery.^{3,4} In enzymology, it is important for the preparation of novel cross-linked enzyme particles for catalysis in aqueous and nonaqueous media.^{5,6} However, a sound scientific basis of the thermodynamic behavior of protein aqueous solutions is still missing. This is needed for understanding phase transformations and optimizing the above applications.

One source of thermodynamic complexity in protein aqueous solutions and their phase transformations is the presence of additives such as salts and polymers. These additives are crucial for inducing phase separation.² Thus protein systems are invariably multicomponent in nature. Understanding and controlling how the concentration of an additive affects the thermodynamic behavior of a protein solution is not only important for phase transformations but also for determining the roles of additives in enzymatic activity and conformational changes.⁷

The chemical potential of the protein component is changed by the concentration of the additive in two ways. First, due to protein–additive net interactions, the additive can modify the

thermodynamic state of the individual protein molecules. This can be described by the protein–chemical-potential derivative with respect to the additive concentration. Second, the additive can modify protein–protein net interactions, i.e., the collective behavior of the protein molecules. This can be described by the effect of the additive on the protein–chemical-potential derivative with respect to protein concentration. These two separate thermodynamic properties may be related to each other only if a microscopic model is introduced. Thus, a microscopic model may be reliable if it accurately describes both of them.

Protein–additive aqueous solutions have been investigated using several experimental techniques. Liquid–liquid partitioning,⁸ equilibrium dialysis,⁹ and ternary diffusion¹⁰ are examples of techniques that have been used to determine protein–additive interactions. However, light scattering,¹¹ X-ray scattering,¹² and self-interaction chromatography¹³ are examples of techniques usually used to determine the effect of additive on protein–protein interactions, mainly through second-virial-coefficient data. The corresponding experimental results have been interpreted by using microscopic models based on preferential hydration (or binding),⁹ DLVO (Derjaguin–Landau–Verwey–Overbeek) interactions,¹⁴ depletion interactions (or crowding),¹⁵ and Donnan effects.¹⁶ However these models, which have been only partially successful, are usually applied to only one of the two aspects.

Among all additives, polyethylene glycol (PEG) is a hydrophilic nonionic polymer used in many biochemical and pharmaceutical applications. Due to its mild action on the biological activity of cell components, PEG is commonly used for liquid–liquid partitioning,¹⁷ the precipitation of biomacromolecules,²

* Author to whom correspondence should be addressed. Phone: (817) 257-6215. Fax: (817) 257-5851. E-mail: O.Annunziata@tcu.edu.

and the preparation of biomaterials.¹⁸ In protein crystallography, PEG is considered the most successful precipitating agent for the production of protein crystals.² Due to the extensive practical use of PEG, it is of fundamental importance to understand the thermodynamic behavior of protein–PEG aqueous solutions.

It is generally believed that the main mechanism of action of PEG on proteins can be described through the influence of mutual volume exclusion on the entropy of the system.^{12,15} This mechanism is usually denoted using the terms: “depletion interactions”¹⁹ or “macromolecular crowding”.²⁰ Models based on depletion interactions have been successful in describing the effect of polymers on model colloidal suspensions especially in relation to their phase transitions.^{21–23} Recently, light²⁴ and X-ray²⁵ scattering measurements have been even used to characterize both protein–protein interactions and protein–PEG interactions. The corresponding results show that depletion–interaction models cannot be used to describe all protein cases.²⁴ Yet, they have been qualitatively successful in describing the effect of PEG molecular weight on the thermodynamic behavior of protein solutions.^{25–28}

To our knowledge, the internal consistency between the experimental results on protein–PEG interactions and those on the effect of PEG concentration on protein–protein interactions has not been quantitatively examined yet. This would be a valuable tool for verifying the validity of existing microscopic models and for developing more accurate ones.

The main objective of this paper is to report an experimental investigation of the liquid–liquid phase separation (LLPS) of aqueous bovine serum albumin (BSA) in the presence of relatively small amounts of PEG with an average molecular weight of 1450 g/mol (PEG1450). LLPS of initially stable protein–PEG–buffer mixtures can be induced when the temperature is lowered. We experimentally characterize two thermodynamically independent properties of the phase boundary: (1) the effect of PEG1450 concentration on the LLPS temperature, (2) BSA/PEG1450 partitioning in the two liquid coexisting phases. We then use thermodynamic perturbation theory to relate the first property to the effects of PEG concentration on protein–protein interactions and the second property to protein–PEG interactions. The reliability of a depletion–interaction model is then examined for this system by investigating its ability to describe both experimental properties. Finally, due to the general importance of LLPS of protein solutions,^{24,27–35} we will also show how phase separation can be induced when the temperature of a protein–PEG–buffer solution is either lowered or increased; i.e., two liquid–liquid phase transitions can be observed for the same mixture.

Thermodynamic Perturbation Theory

We will now outline a thermodynamic perturbation theory that will be used to describe the liquid–liquid phase transition for the protein–polymer–buffer system. This theory, which is an extension of that presented in previous works,^{22,27} will provide the basis for the interpretation of protein–PEG interactions and the effect of PEG concentration on protein–protein interactions.

We describe the composition of this system by the protein molar concentration c_1 and the polymer molar concentration c_2 . The buffer is assumed to be one pseudo-component. To analyze the physical factors that determine protein–polymer interactions and the effect of the polymer on protein–protein interactions, we consider the free energy of the system. As for colloid–polymer mixtures,²² we define the quantity F , representing the difference, at constant volume V and temperature T , between

the Helmholtz free energy of the virtually incompressible protein–polymer–buffer system and the pure buffer system. If the molar volumes of the three components are V_{prot} (for protein), V_{pol} (for polymer), and V_{buff} (for buffer), the change in F due to the replacement (at constant volume) of $V_{\text{prot}}/V_{\text{buff}}$ water moles by one mole of protein and $V_{\text{pol}}/V_{\text{buff}}$ water moles by one mole of polymer are respectively described by the differences of chemical potentials, $\mu_1 = \mu_{\text{prot}} - (V_{\text{prot}}/V_{\text{buff}})\mu_{\text{buff}}$ and $\mu_2 = \mu_{\text{pol}} - (V_{\text{pol}}/V_{\text{buff}})\mu_{\text{buff}}$.²⁷ In this way, it can be shown that the ternary incompressible system may be equivalently treated as a two-component compressible system where the osmotic pressure, Π , becomes the system pressure and μ_1 and μ_2 become the protein and polymer effective chemical potentials, respectively. These quantities will be used to describe the buffer-mediated protein–protein and protein–polymer thermodynamic interactions.

It is convenient to introduce the reduced free energy $\hat{f} = (F - c_1\mu_1^0 - c_2\mu_2^0)/RTV$, where μ_1^0 and μ_2^0 are the standard chemical potentials and R is the ideal gas constant. To a first-order approximation with respect to c_2 , we can write

$$\hat{f}(c_1, c_2, T) = \hat{f}(c_1, T) + c_2 \ln \frac{c_2}{e} + c_2 \left(\frac{\partial \hat{f}^{\text{ex}}}{\partial c_2} \right)_{T, c_1, c_2=0} + \dots \quad (1)$$

where $\hat{f}(c_1, T) \equiv \hat{f}(c_1, 0, T)$ is the reduced free energy for the protein–buffer binary system. The quantities $c_2 \ln(c_2/e)$ and $c_2(\partial \hat{f}^{\text{ex}}/\partial c_2)$ are the contributions to the reduced free energy associated with the replacement of solvent molecules by polymer molecules. The contribution of polymer to the translational entropy of the system is represented by $c_2 \ln(c_2/e)$, whereas $c_2(\partial \hat{f}^{\text{ex}}/\partial c_2)$ is the first term of a series expansion describing the effect of polymer concentration on the excess free energy, \hat{f}^{ex} . For ideal polymer coils, the higher terms of the series disappear.

Although this theory makes no assumption on the nature of the protein–protein and protein–polymer interaction, we will consider the form of eq 1 in the case of the well-established depletion–interaction model.²² For proteins treated as spherical particles in the presence of nonadsorbing polymers, excluded-volume interactions become the only source of thermodynamic nonideality. Due to steric hindrance, the center of mass of a polymer coil is not only excluded from the volume occupied by the protein particles but also from a region surrounding them referred as the depletion layer.²³ The width of this layer is proportional to the gyration radius of the polymer coil. For pure depletion interactions: $\alpha(c_1, T) = \exp(-(\partial \hat{f}^{\text{ex}}/\partial c_2)_{c_1, T, c_2=0})$,²⁷ where α is the volume fraction of the system available to the centers of mass of the polymer coils.

On a model-free basis, we define α as an *apparent* free-volume fraction. We therefore replace $(\partial \hat{f}^{\text{ex}}/\partial c_2)_{c_1, T, c_2=0}$ with $-\ln \alpha$ in eq 1. By differentiating eq 1 with respect to c_1 and c_2 we obtain the following expressions for the reduced chemical potentials and osmotic pressure (to the first order in c_2)

$$\hat{\mu}_1 = \left(\frac{\partial \hat{f}}{\partial c_1} \right)_{c_2, T} = \hat{\mu}'_1(c_1, T) - \frac{c_2}{\alpha} \left(\frac{\partial \alpha}{\partial c_1} \right)_T \quad (2a)$$

$$\hat{\mu}_2 = \left(\frac{\partial \hat{f}}{\partial c_2} \right)_{c_1, T} = \ln \left(\frac{c_2}{\alpha} \right) \quad (2b)$$

$$\hat{\Pi}(c_1, c_2, T) = c_1 \hat{\mu}_1 + c_2 \hat{\mu}_2 - \hat{f} = \hat{\Pi}'(c_1, T) + c_2 - c_1 \frac{c_2}{\alpha} \left(\frac{\partial \alpha}{\partial c_1} \right)_T \quad (2c)$$

where $\hat{\mu}'_1(c_1, T)$ and $\hat{\Pi}'(c_1, T)$ are respectively, the protein reduced chemical potential and the reduced osmotic pressure of the protein–buffer binary system. Equation 2b shows that the thermodynamic activity of the polymer component is represented by the polymer concentration in the free volume: c_2/α .

Protein–polymer thermodynamic interactions can be described by the following cross-derivative²⁷

$$\left(\frac{\partial \hat{\mu}_1}{\partial c_2}\right)_{T, c_1} = \left(\frac{\partial \hat{\mu}_2}{\partial c_1}\right)_{T, c_2} = -\frac{1}{\alpha} \left(\frac{\partial \alpha}{\partial c_1}\right)_T \quad (3)$$

For pure depletion interactions, $(\partial \alpha / \partial c_1)_T$ is negative because the free volume decreases as the protein concentration increases. This implies that $(\partial \hat{\mu}_1 / \partial c_2)_{T, c_1} > 0$, consistent with protein–polymer repulsive interactions.

Protein–protein thermodynamic interactions can be described by the following chemical-potential derivative

$$\left(\frac{\partial \hat{\mu}_1}{\partial c_1}\right)_{T, \mu_2} = \left(\frac{\partial \hat{\mu}'_1}{\partial c_1}\right)_T - \frac{c_2}{\alpha} \left(\frac{\partial^2 \alpha}{\partial c_1^2}\right)_T \quad (4)$$

Equation 4 provides also the basis for the thermodynamic definition of the protein second virial coefficient. For pure depletion interactions, $(\partial^2 \alpha / \partial c_1^2)_T$ is positive because the overlap of depletion layers produces free-volume excess with respect to that of isolated layers. This overlapping increases with protein concentration. This implies that, as the polymer concentration increases, $(\partial \hat{\mu}_1 / \partial c_1)_{T, \mu_2}$ decreases, consistent with a corresponding increase of protein–protein attractive interactions.

In summary, the first derivative $(\partial \alpha / \partial c_1)_T$ is related to protein–polymer interactions while the second derivative $(\partial^2 \alpha / \partial c_1^2)_T$ is related to the effect of polymer concentration on protein–protein interactions. Since $\alpha(c_1, T)$ is, in general, not a free-volume fraction, no assumption on the sign of $(\partial \alpha / \partial c_1)_T$ and $(\partial^2 \alpha / \partial c_1^2)_T$ can be made. Thus protein–polymer repulsive interactions can in principle occur together with a corresponding increase of protein–protein repulsive interaction. This has been shown to be the case for lysozyme–PEG mixtures.^{24,26,36}

We note that the protein–polymer–buffer system has been often described as an effective protein one-component system.^{12,25} According to this description, the polymer effect can be expressed in the form of an effective pair potential in the coordinates of the protein particles. For proteins treated as hard spheres in the presence of nonadsorbing polymers, an attractive depletion potential is generated when the depletion layers of two protein particles overlap.²⁰ However, the pair approximation of this depletion potential is reasonably accurate only at low protein concentrations^{37,38} and, consequently, becomes an acceptable approximation for describing second-virial-coefficient data. At the concentrations relevant to LLPS, it has been shown that this approximation can become a significant source of error.^{37,38} The two-component approach avoids this problem. Furthermore, this approach also can be used to describe the presence of protein/polymer partitioning in the two coexisting liquid phases.

We now consider the liquid–liquid phase transition of the protein–polymer–buffer system. This is described by the LLPS phase boundary $T_{\text{ph}}(c_1, c_2)$. We will show that protein/polymer partitioning between the two liquid phases can be related to protein–polymer interactions while the dependence of T_{ph} on polymer concentration can be related to the effect of polymer concentration on protein–protein interactions.

Protein/polymer partitioning in the two coexisting liquid phases I and II ($c_1^{\text{I}}, c_2^{\text{I}}, c_1^{\text{II}}, c_2^{\text{II}}$) can be examined by considering eq 2b and applying the condition of chemical equilibrium for the polymer component

$$\frac{c_2^{\text{I}}}{\alpha(c_1^{\text{I}}, T)} = \frac{c_2^{\text{II}}}{\alpha(c_1^{\text{II}}, T)} \quad (5)$$

To qualitatively show that the protein/polymer partitioning is related to $(\partial \alpha / \partial c_1)_T$, we perform a power series expansion of eq 5 about the protein critical concentration c_1^c . This yields

$$\ln \frac{c_2^{\text{II}}}{c_2^{\text{I}}} = \frac{1}{\alpha} \left(\frac{\partial \alpha}{\partial c_1}\right)_{T, c_1=c_1^c} (c_1^{\text{II}} - c_1^{\text{I}}) + \dots \quad (6)$$

Equation 6 shows the relation of protein/polymer partitioning to protein–polymer interactions. We comment that our approach neglects the presence of critical fluctuations. Yet, most of our experimental results are far from critical conditions and will be analyzed using eq 5 not eq 6.

The effect of polymer concentration on T_{ph} can be examined by numerically solving the three equilibrium conditions between two liquid phases I and II: $\hat{\mu}_1(\text{I}) = \hat{\mu}_1(\text{II})$, $\hat{\mu}_2(\text{I}) = \hat{\mu}_2(\text{II})$, and $\hat{\Pi}(\text{I}) = \hat{\Pi}(\text{II})$. However an analytical expression relating T_{ph} to $(\partial^2 \alpha / \partial c_1^2)_T$ cannot be determined. To show qualitatively that the dependence of T_{ph} on c_2 is related to $(\partial^2 \alpha / \partial c_1^2)_T$, we will consider the more accessible spinodal condition, $(\partial \hat{\mu}_1 / \partial c_1)_{T=\text{sp}, \mu_2} = 0$. This defines the boundary $T_{\text{sp}}(c_1, c_2)$ between the stable domain and the unstable domain of the system. The effects of polymer concentration on T_{ph} and T_{sp} are closely related because the LLPS boundary is tangent to the spinodal boundary.³⁴

For pure excluded-volume interactions, eq 4 predicts that, as the polymer concentration increases, $(\partial \hat{\mu}_1 / \partial c_1)_{T, \mu_2}$ decreases and can be made to reach zero. Thus sufficient polymer can be used to bring the protein–polymer–buffer system to the spinodal boundary. This is a sufficient condition for LLPS to occur.

Protein–protein net attraction energy drives LLPS.³⁹ We however observe that LLPS of the protein–buffer binary system rarely has been reported^{34,40} in the experimentally accessible temperature domain (~ 260 – 320 K). One reasonable hypothesis is that this attraction is usually weak for water-soluble proteins. This implies that protein–buffer systems (with attraction) would usually behave as “supercritical fluids” in the accessible temperature domain. This observation allows us to conclude that the following high-temperature series expansions can be written for $\hat{f}'_1(c_1, T)$ and $\alpha(c_1, T)$

$$\hat{f}'_1(c_1, T) = \hat{f}'^{(0)}(c_1) + \hat{f}'^{(1)}(c_1) \frac{1}{RT} + \hat{f}'^{(2)}(c_1) \left(\frac{1}{RT}\right)^2 + \dots \quad (7a)$$

$$\alpha(c_1, T) = \alpha^{(0)}(c_1) + \alpha^{(1)}(c_1) \frac{1}{RT} + \alpha^{(2)}(c_1) \left(\frac{1}{RT}\right)^2 + \dots \quad (7b)$$

In eq 7a, $\hat{f}'^{(1)}(c_1)$ represents the internal energy (per unit volume) of the protein–buffer binary system to the first order in $1/RT$. This quantity is negative in the presence of protein–protein weak attraction energy. We comment that eq 7a may fail to describe the LLPS boundary of the binary protein–buffer system, which would be located at relatively low temperatures.

If we insert eqs 7a and 7b into eq 4 and apply the spinodal condition, then we obtain to the first order

$$\frac{1}{T_{sp}} = -R \frac{(d^2\hat{f}^{(0)}/dc_1^2)}{(d^2\hat{f}^{(1)}/dc_1^2)} \left[1 - \frac{(d^2\alpha^{(0)}/d^2c_1)/\alpha^{(0)}}{(d^2\hat{f}^{(0)}/d^2c_1)} c_2 \right] + \dots \quad (8)$$

Equation 8 shows how the dependence of T_{sp} on polymer concentration is related to the effect of polymer concentration on protein-protein interactions. For our protein-buffer system, $(d^2\hat{f}^{(0)}/dc_1^2) > 0$ due to protein-protein hard-core repulsion,²² and $(d^2\hat{f}^{(1)}/dc_1^2) < 0$ due to the protein-protein attraction energy.²⁷ Thus, T_{sp} is expected to increase with polymer concentration for pure depletion interactions.

Although this thermodynamic perturbation theory makes no assumption on the nature of microscopic interactions, there are two important limitations to take into account. These are: (1) the buffer is regarded as one pseudo-component; (2) polymer-polymer interactions are not taken into account. We will discuss these two limitations in the following sections.

Materials and Methods

Materials. Bovine serum albumin (BSA) was purchased from Sigma (purity 99%). The molecular weight was assumed to be 66.4 kg/mol. High-performance liquid chromatography (HPLC, System Gold, Beckman Coulter) with a size-exclusion column (Biosep-SEC-S 2000, Phenomenex) shows the presence of 20% BSA oligomers. Thus further purification of BSA was performed using size-exclusion preparative chromatography. The column was packed using Sephacryl S-200 purchased from Amersham Biosciences. The mobile phase was a sodium phosphate buffer (0.05 M, pH 7.1), and the flow rate was 1.5 mL/min. The BSA monomer fraction was collected and stored at -4 °C. Size-exclusion HPLC on the monomer fraction showed the purity to be greater than 99%. Polyethylene glycol (PEG) with average molecular weights of 1.45 kg/mol (PEG1450) and 8.0 kg/mol (PEG8000) were purchased from Acros Chemicals and used without further purification.

BSA-PEG1450-buffer solutions were prepared as follows. The purified BSA was dialyzed exhaustively (Amicon, Millipore) into sodium acetate aqueous buffer (0.1 M, pH 5.2). Solutions containing dilute BSA in acetate buffer were concentrated by centrifugation (3500g, Allegra 25R, Beckman Coulter) using ultrafiltration devices (Centricon YM-30, Millipore). When the target protein concentration was reached, a known weight of PEG1450 was added to the protein solution. (Weight measurements were performed using a AT 400 Mettler-Toledo balance.) The concentration of BSA in the samples was determined by UV absorption at 278 nm (DU 800 spectrophotometer, Beckman Coulter), using the extinction coefficient value of $0.667 \text{ mg}^{-1} \text{ mL cm}^{-1}$.⁴¹ The concentration of PEG1450 in the samples was calculated by using the mass of PEG and the total volume of the solution. The total volume was calculated from the sample mass using the corresponding specific volume, i.e., 0.735 mL/g for the protein,⁴² 0.84 mL/g for PEG,²⁴ and 1.000 mL/g for the buffer (the buffer density was measured using a DMA40 Mettler-Paar density meter) as in previous work.^{27,28} BSA-PEG8000-buffer solutions were prepared in the same way. The only difference is that sodium phosphate aqueous solution (0.2 M, pH 7.1) was used as a buffer.

Measurements of LLPS Temperature. The LLPS temperature, T_{ph} , for a given protein-PEG-buffer sample was determined by measuring sample turbidity as a function of temperature. A turbidity meter was built by using a programmable circulating bath (1197P, VWR) connected to a homemade optical cell where the sample is located. The temperature at the sample location was measured by using a calibrated thermo-

couple (± 0.1 °C). Light coming from a solid-state laser (633 nm, 5 mW, Coherent) goes through the sample, and the transmitted intensity, I , is measured using a photodiode detector and a computer-interfaced optical meter (1835-C, Newport). For a given transparent sample, the transmitted intensity, I_0 , was measured. The temperature of the water bath was slowly decreased (0.5 °C/min), and the temperature T_{cloud} at which the turbidity (given by $\log(I_0/I)$) has an inflection point was taken. When $I \approx 0$, the water bath temperature was increased at the same rate, and the temperature T_{clear} at which the turbidity has an inflection point was taken. The temperature reported for the onset of LLPS was $T_{ph} = (T_{cloud} + T_{clear})/2$ as recommended in previous work.⁴³ Five $T_{ph}(c_2)$ curves at constant c_1 were obtained. The samples for a given curve were prepared by mixing two stock solutions having the same protein concentrations but different PEG concentrations.

Measurements of Protein/PEG Partitioning. The two coexisting phases were obtained by quenching a sample at a fixed temperature below the LLPS temperature as described in previous work.^{27,28} The samples were left at the established temperature for approximately 1 day. The opaque samples were then inserted in Teflon test tube holders thermally equilibrated at exactly the same temperature and promptly located in a centrifuge thermally equilibrated at approximately the same temperature (± 1 °C). After centrifugation (1000g, 5 min), two liquid phases separated by a meniscus were obtained. The sample test tubes used in these experiments can be opened from both the top and the bottom. A fraction of the protein-dilute phase (far from the liquid-liquid interface) was taken from the test tube top aperture, while a fraction of the protein-concentrate phase was taken from the test tube bottom aperture. This procedure avoids cross-contamination. The protein concentration in each phase was determined by UV absorption. The concentration of PEG1450 in each aliquot was determined by using a standardized refractive-index detector (RI-2031, Jasco). Separation of PEG1450 from BSA was achieved by isocratic elution of the mixture on a size-exclusion HPLC column (Superdex 75, Amersham Biosciences). Sodium acetate buffer (0.01 M, pH 5.2) was used as the mobile phase with a flow rate of 0.6 mL/min. The procedure was verified with protein-PEG aqueous solutions of known compositions showing that the error in PEG concentration was less than 5%. In all cases, the measured protein and PEG concentrations in the two coexisting phases were consistent with the protein and PEG concentrations in the original homogeneous samples.

Measurements of Light-Scattering. Measurements of static light-scattering were performed at 25.0 ± 0.1 °C. All protein samples were filtered through a $0.02 \mu\text{m}$ filter (Anotop 10, Whatman) and placed in a test tube. The experiments were performed on a light-scattering apparatus built using the following main components: He-Ne laser (35 mW, 632.8 nm, Coherent Radiation), manual goniometer and thermostat (Photocor Instruments), multi-tau correlator, APD detector and software (PD4042, Precision Detectors). All measurements were performed at a scattering angle of 90° . The second virial coefficient,⁴⁴ B_2 , was obtained from $kc_1/R_{90^\circ} = 1/M_{prot} + 2B_2c_1$, where $k = 4\pi^2 n_0^2 (dn/dc_1)^2 / (N_A \lambda^4)$, n_0 is the refractive index of the buffer, (dn/dc_1) is the refractive-index increment associated with c_1 (in mg/mL), N_A is the Avogadro's number, λ is the laser wavelength in vacuum, R_{90° is the excess Rayleigh ratio at 90° , and M_{prot} is the protein molecular weight. The values of R_{90° were obtained from $R_{90^\circ} = (I_s - I_{s,0})/I_{s,R}(n_0^2/n_R^2)R_{90^\circ,R}$, where I_s is the scattered intensity of the solution, $I_{s,0}$ is the scattered intensity of the buffer, $I_{s,R}$ is the scattering intensity of toluene

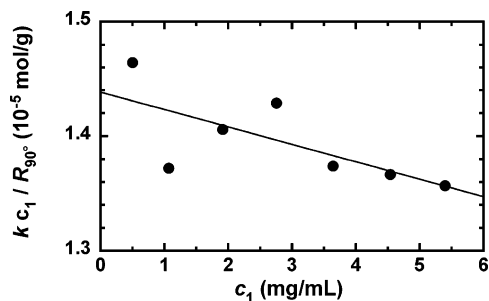


Figure 1. Static light-scattering data for the BSA–acetate buffer system at pH 5.2 and 298.15 K. The second-virial-coefficient value, B_2 , is $-0.1 \pm 0.1 \times 10^{-4} \text{ mL mol g}^{-1}$, $kc_1/R_{90^\circ} = 1/M_{\text{prot}} + 2Bc_1$ (see the Materials and Methods section for details).

(the standard), and n_R and $R_{90^\circ, R}$ are, respectively, the available refractive index and the Rayleigh ratio of toluene.⁴⁵ As a diagnostic, correlation functions were also analyzed using a regularization algorithm (Precision Deconvolve 32, Precision Detectors) to confirm protein monodispersity.

Results

The chosen buffer for the studies on the BSA–PEG1450 mixtures was a 0.1 M sodium acetate aqueous solution at pH 5.2. At this pH, BSA is close to its isoelectric point.⁴⁶ Since the protein net charge is nearly zero, Donnan effects with sodium acetate and protein–protein repulsive electrostatic interactions should not be significant. This also suggests that the amount of PEG1450 required to induce LLPS at this pH is close to the minimum.

To characterize protein–protein interactions in the protein–buffer binary system, we determine the value of its second virial coefficient, B_2 , at 298.15 K. In Figure 1, we report static light-scattering measurements on the BSA–buffer binary system. We find that $B_2 = -0.1 \pm 0.1 \times 10^{-4} \text{ mL mol g}^{-1}$. The value calculated for the corresponding hard-sphere system is $0.44 \times 10^{-4} \text{ mL mol g}^{-1}$. Thus our results provide a strong indication that the protein–protein interactions are attractive in this binary system. However, protein–buffer systems do not undergo LLPS within the experimental temperature range, 260–310 K, and for protein concentrations as high as 400 mg/mL. This is consistent with the hypothesis that the binary system behaves as a supercritical fluid. Upon the addition of PEG1450 (20–80 mg/mL), LLPS is observed within the experimental temperature domain.

In Figure 2, we report our measurements of LLPS temperature, T_{ph} , as a function of PEG1450 concentration, c_2 , at five constant BSA concentrations, c_1 around the protein critical concentration (here in mg/mL), $c_1^c \approx 240 \text{ mg/mL}$. This value of c_1^c was obtained from BSA/PEG1450 partitioning measurements shown later. In all five cases, the LLPS temperature increases with PEG1450 concentration. According to eq 8, this result is consistent with (1) the protein–protein interaction energy being attractive in the protein–buffer binary system and (2) the PEG1450 concentration increasing protein–protein attractive interactions. The first effect is in agreement with our B value while the second effect is expected in the presence of depletion interactions. We also observe that T_{ph} increases with c_1 for all of our PEG1450 concentrations (Figure 2). This implies that $(\partial T_{\text{ph}}/\partial c_1)_{c_2} > 0$. Since $(\partial T_{\text{ph}}/\partial c_1)_{c_2} = -(\partial T_{\text{ph}}/\partial c_2)_{c_1}(\partial c_2/\partial c_1)_{T_{\text{ph}}}$,²⁷ we conclude that $(\partial c_2/\partial c_1)_{T_{\text{ph}}} < 0$ around the critical protein concentration. This is consistent with the presence of significant BSA/PEG1450 partitioning. Similar results were also obtained for γ -crystallin–PEG aqueous mixtures.^{27,28}

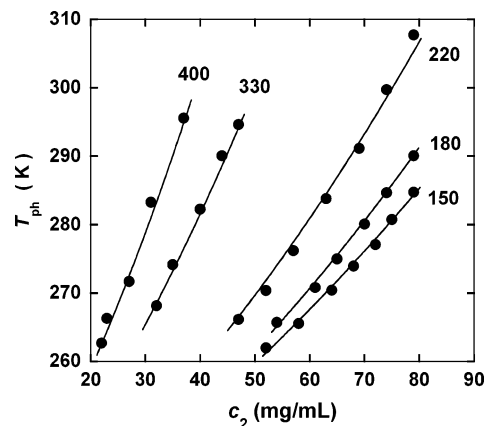


Figure 2. LLPS temperature, T_{ph} , as a function of PEG1450 concentration, c_2 , at five constant BSA concentrations, c_1 . The solid curves represent our calculated values obtained by applying equilibrium conditions to eqs 2a–c as described in the Discussion section. The numbers associated with each curve identify the corresponding value of c_1 in mg/mL.

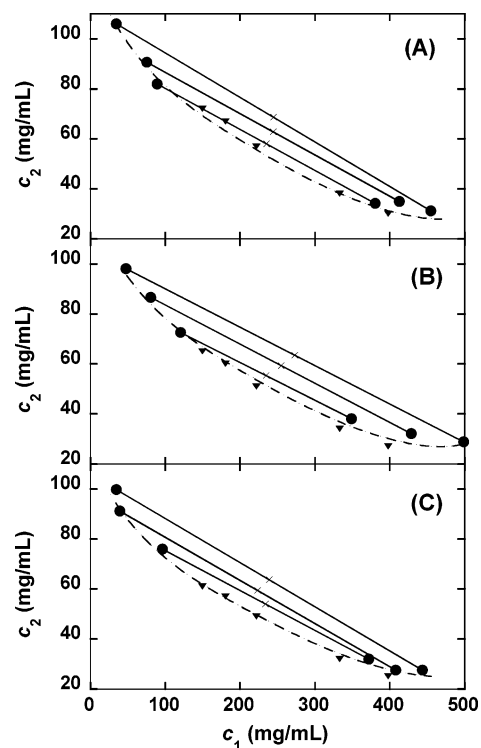


Figure 3. Measurements of BSA/PEG1450 partitioning ($c_1^I, c_2^I, c_1^{II}, c_2^{II}$) at three different temperatures: (A) 278, (B) 271, and (C) 268 K. The straight lines (tie lines) connect the pairs of points representing the coexisting phases (●). The crosses (×) represent the average composition of the coexisting phases. The triangles (▼) represent the values of (c_1, c_2) extracted by interpolation of our $T_{\text{ph}}(c_1, c_2)$ values of Table 1. The dashed curves are guides for the eye.

In Figure 3, we report measurements of BSA/PEG1450 partitioning ($c_1^I, c_2^I, c_1^{II}, c_2^{II}$) performed at three different temperatures. The straight lines (tie lines), which connect the pairs of points representing the coexisting phases, show that there is a large difference in polymer concentration between the two phases. We also find that this difference is still significant if we report the PEG concentrations with respect to the buffer volume, calculated by removing the volumetric contribution of the protein component. This is consistent with the presence of BSA–PEG repulsive interactions as expected for depletion interactions. We have used our measurements of BSA/PEG1450

partitioning to estimate the protein critical concentration, c_c^c , by simply averaging the two concentrations c_1^I and c_1^{II} . (The concentration values are available in the Supporting Information.) We estimate the critical concentration to be 240 ± 20 mg/mL, corresponding to a volume fraction of $\phi_c = 0.18 \pm 0.01$.

In Figure 3, we also report values of (c_1, c_2) extracted by interpolation of our $T_{ph}(c_1, c_2)$ results of Figure 2. The overall agreement between the two sets of data can be considered satisfactory. However, a small discrepancy is observed in our results at high protein concentrations, where the (c_1^{II}, c_2^{II}) points appear to be located at lower c_1 and higher c_2 values than those predicted from the values of $T_{ph}(c_1, c_2)$. Due to the high viscosity of the protein-concentrate phase, the mechanical separation of residual protein-dilute phase from the protein-concentrate phase may be difficult to achieve. We thus expect that the protein-concentrate phases may still contain small amounts ($\sim 10\%$) of the protein-dilute phase. As we will discuss later, this will not be a significant source of errors in our quantitative examination of the BSA–PEG1450 interactions.

We now examine our assumption that the buffer can be regarded as one pseudo-component. This assumption is valid if the internal composition of the buffer is the same in all of our experiments. For our $T_{ph}(c_1, c_2)$ measurements, the concentration of buffer solutes inside the buffer volume is indeed kept the same. However, in the two coexisting phases (c_1^I, c_2^I) and (c_1^{II}, c_2^{II}) , the thermodynamic activity of buffer solutes is the same. Thus the buffer can be approximately treated as one pseudo-component if the difference of the buffer solute concentrations in the two coexisting phases is small. This is corroborated by the observed agreement between the two sets of data in Figure 3.

Discussion

The thermodynamic behavior of the BSA–PEG1450–buffer system can be examined by applying the above-described thermodynamic perturbation theory to our experimental results. Our approach will be to use an expression for $\alpha(c_1, T)$ able to describe our two sets of data. Since both sets of data are consistent with the presence of depletion interactions, we will use an expression of $\alpha(c_1, T)$ that represents the free-volume fraction. The dependence of the free-volume fraction on the thickness of the depletion layer is taken into account by introducing the ratio $q = \delta/R_{prot}$, where R_{prot} is the average radius of the protein and δ is the thickness of the depletion layer.^{22,23,26,27} However, the parameter q is not calculated from microscopic parameters but is determined using our experimental results. Specifically, we will determine a first value of q from our measurements on BSA/PEG1450 partitioning and a second value of q from our measurements on LLPS temperature. The agreement between these two values of q will be used as criteria to establish if depletion–interaction models satisfactorily describe both BSA–PEG1450 interactions and the effect of PEG1450 concentration on protein–protein interactions. An attempt will be also made to compare the determined values of q with that calculated from microscopic parameters. However, this second comparison is not very reliable due to the simplifications involved in the chosen expression for $\alpha(c_1, T)$ and $\hat{f}_1(c_1, T)$.

For α , we will use an expression that treats proteins as hard spheres. From scaled particle theory⁴⁷ applied to hard spheres, the following expression as been determined²²

$$\alpha = \alpha^{(0)} = (1 - \phi) \exp(-A\eta - B\eta^2 - C\eta^3) \quad (9)$$

where $\phi = V_{prot}c_1$, $\eta = \phi/(1 - \phi)$, $A = 3q + 3q^2 + q^3$, $B = 4.5q^2 + 3q^3$, $C = 3q^3$. Computer simulations show that eq 9 is reasonably accurate even for very dense hard-sphere fluids.³⁷ We comment that, when ϕ is small, the overlapping of the depletion layers can be neglected and eq 9 becomes $\alpha \approx 1 - (1 + q)^3\phi$. This is true even when $\alpha^{(1)}$ and higher-order terms are included.

A set of apparent q values is determined from the partitioning measurements by applying eqs 5 and 9 to the $(c_1^I, c_2^I, c_1^{II}, c_2^{II})$ values. The results are available as Supporting Information for each pair of coexisting phases. No dependence of q on temperature and the average PEG concentration, \bar{c}_2 , could be observed within the experimental error. We thus report the average value: $q = 0.35 \pm 0.03$. We note that the q values calculated by using $\alpha \approx 1 - (1 + q)^3\phi$ are only 10–15% smaller than the values calculated using eq 9. We thus conclude that the overlapping of the depletion layers contributes only marginally to our q values. This also indicates that our omission of $\alpha^{(1)}$ and higher-order terms in eq 9 is a reasonable approximation.

As mentioned in the Results section, the protein-concentrate phases may still contain small amounts of the corresponding protein-dilute phases. However, we observe that, according to $\alpha \approx 1 - (1 + q)^3\phi$, even a large contamination has no effect on the obtained value of q . According to the complete eq 9, we estimate that 10% of the dilute phase would produce a small increase in the q values (2–4%). We therefore conclude that contamination does not significantly change our final results.

The apparent q values are determined from the measurements of LLPS temperature by comparing our results in Figure 2 with the LLPS phase boundary computed by applying the three equilibrium conditions to eqs 2a–c. However this requires not only an expression for $\alpha(c_1, T)$ but also one for $\hat{f}(c_1, T)$. For $\hat{f}(c_1, T)$, we consider eq 7a applied to hard spheres interacting by square-well potentials with well magnitude ϵ and range of interaction λ . The expression for $\hat{f}^{(0)}(\phi)$ is given by the Carnahan–Starling equation,⁴⁸ which has shown to be very accurate even for very dense hard-sphere fluids

$$\hat{f}^{(0)}(\phi) = c_1 \ln \frac{c_1}{e} + c_1 \frac{\phi(4 - 3\phi)}{(1 - \phi)^2} \quad (10)$$

The expressions for $\hat{f}^{(1)}(\phi)/\epsilon$ and $\hat{f}^{(2)}(\phi)/\epsilon^2$ depend on the choice of λ . According to the model of the square-well potential, $\phi_c = 0.18 \pm 0.01$ corresponds to $\lambda \approx 1.5$.³⁹ We thus consider the corresponding expressions at $\lambda = 1.5$.⁴⁹ These are described in the Appendix. We remark that, according to eq 8 and a numerical analysis of the LLPS boundary, the obtained value of q is significantly affected only by the choice of $\hat{f}^{(0)}(\phi)$. This quantity, contrary to $\hat{f}^{(1)}(\phi)$ and $\hat{f}^{(2)}(\phi)$, does not depend on the nature of the interaction potential. We also observe that the choice of $\hat{f}^{(0)}(\phi)$ and $\alpha^{(0)}(\phi)$ must be consistent with respect to each other since the accuracy of their second-derivative ratio is crucial for the determination of q (see eq 8).

For given values of T_{ph} and $\hat{\mu}_2$, we obtain c_1^I and c_1^{II} by numerically solving the conditions

$$\hat{\mu}_1(c_1^I, \hat{\mu}_2, T_{ph}) = \hat{\mu}_1(c_1^{II}, \hat{\mu}_2, T_{ph}) \quad (11a)$$

$$\hat{\Pi}(c_1^I, \hat{\mu}_2, T_{ph}) = \hat{\Pi}(c_1^{II}, \hat{\mu}_2, T_{ph}) \quad (11b)$$

The corresponding values of c_2^I and c_2^{II} are obtained by applying eq 3b. The phase boundary is then computed by repeating this procedure for several values of T_{ph} and $\hat{\mu}_2$. Finally

TABLE 1: Values of ϵ and q

c_1 (mg/mL)	ϵ/R (K)	q
150	172	0.31
180	168	0.31
220	168	0.31
330	181	0.31
400	198	0.31

a $T_{ph}(c_2)$ curve is generated for the chosen value of c_1 by interpolation. The comparison between the experimental data and the calculated curves (solid lines in Figure 2) has allowed us to determine q and ϵ .

Our results of q and ϵ for each experimental c_1 value are reported in Table 1. We observed that changes in the reported q values larger than 0.01 produce a noticeable discrepancy between the experimental data and the theoretical curves for all ϵ values. We therefore obtain the same value of q in all five cases and report $q = 0.31 \pm 0.01$. That q does not depend on c_1 is strong evidence that the chosen expressions for $\hat{f}^{(0)}(\phi)$ and $\alpha^{(0)}(\phi)$ are satisfactory. However, the value of ϵ is found to increase with c_1 at the highest protein concentrations. This observed discrepancy can be attributed to the nonsufficient accuracy in the chosen expressions for $\hat{f}^{(1)}(\phi)$ and $\hat{f}^{(2)}(\phi)$.

Our analysis shows that the agreement on q between the two sets of data is good. This implies that the depletion–interaction model satisfactorily describes the BSA–PEG1450–buffer system. Thus eq 9 with $q \approx 0.3$ can be used to describe both BSA–PEG1450 interactions (from eq 3) and the effect of PEG1450 concentration on protein–protein interactions (from eq 4).

As already mentioned, the thermodynamic perturbation theory described above neglects the presence of polymer–polymer interactions. These interactions should be included for a more general and accurate description of our system. We also note that this approximation may become rather inadequate if coil–coil interpenetration is significant. For polymers, the concentration at which this interpenetration starts to be important marks the passage from their dilute regime to their semidilute regime. For PEG1450, this transition occurs at $c_2 \approx 100$ mg/mL.⁵⁰ Thus our experimental PEG concentrations fall inside the dilute-regime domain. We however observe that polymer–polymer interactions in our ternary system cannot be simply approximated with those of the corresponding PEG1450–buffer system. This would ignore the effect of BSA concentration on polymer–polymer interactions, which is expected to be significant due to the high protein concentration of our mixtures. Thus, as criteria to evaluate the importance of polymer–polymer interactions, we will directly consider our ternary mixtures. We observe that our measurements on the LLPS temperature, which are performed on a wide range of PEG1450 concentrations, can be accurately described by the same value of $q = 0.31$. This indicates that our results do not significantly depend on PEG1450 concentration. This would not be consistent with a significant presence of PEG–PEG interactions. We thus believe that neglecting the presence of polymer–polymer interactions does not significantly affect our conclusions.

We make an attempt to compare the determined value of $q \approx 0.3$ with that obtained from microscopic structural parameters. The value of q is given by $q = \delta/R_{prot} = kR_g/R_{prot}$, where R_g is the radius of gyration of the polymer and k is a parameter function itself of R_g/R_{prot} due to polymer deformability. We estimate $R_{prot} = 2.7$ nm for BSA from the specific volume and molecular weight of the protein and calculate $R_g = 1.5$ nm for PEG1450 from the known dependence of R_g on PEG molecular

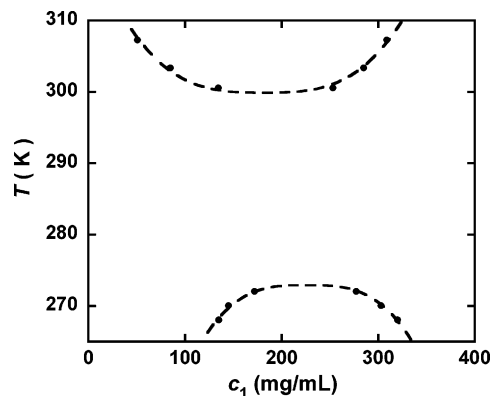


Figure 4. Two coexistence curves of the ternary mixture with the composition: BSA, 200 mg/mL; PEG8000, 70 mg/mL; sodium phosphate buffer, pH 7.1, 0.2 M. The points were determined by measuring the protein concentration in the two coexisting phases at several temperatures. The solid curves are guides for the eye.

weight.²⁶ For our R_g/R_{prot} value, computer simulations and theoretical modeling indicate that $k \approx 1$,^{51,52} yielding therefore $q \approx 0.6$. This discrepancy can be related to several microscopic details such as the actual shape of the protein molecules, the conformational properties of PEG coils, and the presence of protein–PEG weak attraction. A similar discrepancy was also observed for other protein–PEG mixtures.^{26–28} However the value of q for these systems was only obtained from measurements of protein/PEG partitioning. We also make an attempt to estimate the value of ϵ from our experimental value of B . For the square-well potential, $BM_{prot}^2/V_{prot} = 4 - 4[\exp(\epsilon/RT) - 1](\lambda^3 - 1)$.⁵³ This equation yields $\epsilon/R = 120$ K for $\lambda = 1.5$. Considering all approximations involved, this value is not very different from those reported in Table 1.

LLPS of Protein–PEG–Buffer Mixtures. The experimental results reported in the previous section show that LLPS may be induced if the temperature of a protein–PEG–buffer mixture is lowered below the corresponding phase boundary. The presence of this phase transition can be predicted by a thermodynamic perturbation theory that treats the buffer as one pseudo-component and neglects polymer–polymer interactions. These two factors, which may not be ignored for high concentrations of buffer solutes or high PEG molecular weights, can bring about a more complex phase-transition behavior. As an example, we consider the mixture prepared by using BSA (200 mg/mL), PEG8000 (70 mg/mL), and sodium phosphate buffer (0.2 M, pH 7.1). This mixture undergoes LLPS not only by lowering the temperature below 273 K but also by increasing it above 300 K. For this mixture, we determine the two coexistence curves shown in Figure 4. We also find (data not shown) that a small increase in phosphate concentration significantly reduces the temperature gap between the two boundaries.

The coexistence curve with the upper critical point can be qualitatively described by invoking the same factors used to explain the BSA–PEG1450–acetate buffer system. However, the coexistence curve with a lower critical point can be explained by considering the corresponding PEG8000–phosphate buffer mixture. For this system, LLPS with a lower critical point is also observed when the temperature is increased above 363 K, consistent with previous results.⁵⁴ Thus the effect of BSA is to move this phase boundary toward lower temperatures. Since this phase transition is driven by the PEG–buffer system, a wide range of protein systems can undergo LLPS when the temperature is increased.

We remark that two LLPS boundaries may be a valuable tool for protein crystallization and biomaterials science in general. For instance, since it is believed that critical fluctuations³³ enhance the nucleation of protein crystals, the presence of two critical points can extend the composition domain where critical fluctuations would occur. This could be used for optimizing protein crystallization.

Summary and Conclusions

We have examined the thermodynamic behavior of the BSA-PEG1450-buffer system using LLPS measurements. For this system, we have experimentally determined the effect of PEG concentration on the LLPS temperature and protein/PEG partitioning in the two coexisting phases. Our results were interpreted using a thermodynamic perturbation theory. Using this theory, we have found that a depletion-interaction model satisfactorily explains both protein-PEG interactions and the effect of PEG concentration on protein-protein interactions for our system. We believe that the parallel examination of these two thermodynamic properties is a valuable tool for verifying the reliability of existing models and for developing more accurate ones. Finally, we have shown that protein-PEG-buffer mixtures can also exhibit two distinct liquid-liquid phase transitions.

Appendix

According to second-order perturbation theory, the compressibility factor, z , can be written as

$$z' = z^{(0)} + z^{(1)} \frac{1}{RT} + z^{(2)} \left(\frac{1}{RT} \right)^2$$

The square-well potential, $V(r)$, is given by

$$V(r) = \begin{cases} \infty & \text{for } r < \sigma \\ -\epsilon & \text{for } \sigma \leq r \leq \lambda\sigma \\ 0 & \text{for } r > \lambda\sigma \end{cases}$$

where σ is the hard-core diameter, λ is a measure of the well width, and ϵ is the well depth. The expression for $z^{(0)}$ is given by the Carnahan-Starling equation of state

$$z^{(0)} = \frac{1 + \phi + \phi^2 - \phi^3}{(1 - \phi)^3}$$

The expressions for $z^{(1)}$ and $z^{(2)}$ at $\lambda = 1.5$ are

$$z^{(1)}/\epsilon = \frac{-9.5\phi \left(1 - 1.13086\phi - 5.72921\phi^2 + 9.50043\phi^3 - 2.37511\phi^4 \right)}{(1 - \phi)^4}$$

$$z^{(2)}/\epsilon^2 = -492.36296\phi^2 \frac{2 - 12.31907\phi}{(1 + 8.26765\phi)^4}$$

Analytical expressions for $\hat{f}^{(1)}(\phi)$ and $\hat{f}^{(2)}(\phi)$ are obtained by applying

$$\hat{f} = c_1 \ln \left(\frac{c_1}{e} \right) + c_1 \int_0^{\phi} [(z' - 1)/\phi] d\phi$$

Acknowledgment. This work was supported by Texas Christian University Research and Creative Activity Funds.

Supporting Information Available: LLPS temperatures for the BSA-PEG1450-buffer system and BSA/PEG1450 parti-

tioning results. This material is available free of charge via the Internet at <http://pubs.acs.org>.

References and Notes

- Chayen, N. E. *Curr. Opin. Struct. Biol.* **2004**, *14*, 577.
- McPherson, A. *Crystallization of Biological Macromolecules*; Cold Spring Harbor Laboratory Press: New York, 1998.
- Patil, G. V. *Drug Dev. Res.* **2003**, *58*, 219.
- Bromberg, L.; Rashba-Step, J.; Scott, T. *Biophys. J.* **2005**, *89*, 3424.
- Roy, J. J.; Abraham, T. E. *Chem. Rev.* **2004**, *104*, 3705.
- Schevaart, R.; Wolbers, M. W.; Golubovic, M.; Ottens, M.; Kieboom, A. P. G.; van Rantwijk, F.; van der Wielen, L. A. M.; Sheldon, R. A. *Biotechnol. Bioeng.* **2004**, *20*, 754.
- Ru, M. T.; Hirokane, S. Y.; Lo, A. S.; Dordick, J. S.; Reimer, J. A.; Clark, D. S. *J. Am. Chem. Soc.* **2000**, *122*, 1565.
- Abbott, N. L.; Blankshtein, D.; Hatton, T. A. *Macromolecules* **1991**, *24*, 4334.
- Arakawa, T.; Bhat, R.; Timasheff, S. N. *Biochemistry* **1990**, *29*, 1914.
- Annunziata, O.; Paduano, L.; Pearlstein, A. J.; Miller, D. G.; Albright, J. G. *J. Phys. Chem. B* **2006**, *110*, 1405.
- Curtis, R. A.; Ulrich, J.; Montaser, A.; Prausnitz, J. M.; Blanch, H. W. *Biotechnol. Bioeng.* **2002**, *79*, 367.
- Tardieu, A.; Bonnete, F.; Finet, S.; Vivares, D. *Acta Crystallogr., Sect. D: Biol. Crystallogr.* **2002**, *58*, 1549.
- Tessier, P. M.; Lenhoff, A. M.; Sandler, S. I. *Biophys. J.* **2002**, *82*, 1620.
- Tardieu, A.; Le Verge, A.; Malfois, M.; Bonnete, F.; Finet, S.; Ries-Kautt, M.; Belloni, L. *J. Cryst. Growth* **1999**, *196*, 193.
- Adams, M.; Fraden, S. *Biophys. J.* **1998**, *74*, 669.
- Annunziata, O.; Paduano, L.; D. G.; Albright, J. G. *J. Phys. Chem. B* **2006**, *110*, 16139.
- Albertsson, P. Å. *Partition of Cell Particles and Macromolecules*; Wiley: New York, 1986.
- Roberts, M. J.; Bentley, M. D.; Harris, J. M. *Adv. Drug. Delivery Rev.* **2002**, *54*, 459.
- Kulkarni, A. M.; Chatterjee, A. P.; Schweizer, K. S.; Zukoski, C. F. *Phys. Rev. Lett.* **1999**, *83*, 4554.
- Hall, D.; Minton, A. P. *Biochim. Biophys. Acta* **2003**, *1649*, 127.
- Asakura, S.; Oosawa, F. *J. Chem. Phys.* **1954**, *22*, 1255.
- Lekkerkerker, H. N. W.; Poon, W. C. K.; Pusey, P. N.; Stroobants, A.; Warren, P. B. *Europhys. Lett.* **1992**, *20*, 559.
- Ilett, S. M.; Orrock, A.; Poon, W. C. K.; Pusey, P. N. *Phys. Rev. E* **1995**, *51*, 1344.
- Bloustone, J.; Virmani, T.; Thurston, G. M.; Fraden, S. *Phys. Rev. Lett.* **2006**, *96*, 087803.
- Vivares, D.; Belloni, L.; Tardieu, A.; Bonnete, F. *Eur. Phys. J. E* **2002**, *9*, 15.
- Bhat, R.; Timasheff, S. N. *Protein Sci.* **1992**, *1*, 1133.
- Annunziata, O.; Asherie, N.; Lomakin, A.; Pande, J.; Ogun, O.; Benedek, G. B. *Proc. Natl. Acad. Sci. U.S.A.* **2002**, *99*, 14165.
- Annunziata, O.; J.; Ogun, O.; Benedek, G. B. *Proc. Natl. Acad. Sci. U.S.A.* **2003**, *100*, 970.
- Galkin, O.; Vekilov, P. G. *Proc. Natl. Acad. Sci. U.S.A.* **2000**, *97*, 6277.
- Gliko, O.; Neumaier, N.; Pan, W.; Haase, I.; Fischer, M.; Bacher, A.; Weinkauf, S.; Vekilov, P. G. *J. Am. Chem. Soc.* **2005**, *127*, 3433.
- Stradner, A.; Sedgwick, H.; Cardinaux, F.; Poon, W. C. K.; Egelhaaf, S. U.; Schurtenberger, P. *Nature* **2004**, *432*, 492.
- Anderson, V. J.; Lekkerkerker, H. N. W. *Nature* **2002**, *416*, 811.
- ten Wolde, P. R.; Frenkel, D. *Science* **1997**, *277*, 1975.
- Broide, M. L.; Berland, C. R.; Pande, J.; Ogun, O.; Benedek, G. B. *Proc. Natl. Acad. Sci. U.S.A.* **1991**, *88*, 5660.
- Pande, A.; Pande, J.; Asherie, N.; Lomakin, A.; Ogun, O.; King, J. A.; Lubsen, N. H.; Walton, D.; Benedek, G. B. *Proc. Natl. Acad. Sci. U.S.A.* **2000**, *97*, 1993.
- Vergara, A.; Capuano, F.; Paduano, L.; Sartorio, R. *Macromolecules* **2006**, *39*, 4500.
- Gast, A. P.; Hall, C. K.; Russell, W. B. *J. Colloid Interface Sci.* **1983**, *96*, 251.
- Meijer, E. J.; Frenkel, D. *J. Chem. Phys.* **1994**, *100*, 6873.
- Lomakin, A.; Asherie, N.; Benedek, G. B. *J. Chem. Phys.* **1996**, *104*, 1646.
- Taratuta, V. G.; Holschbach, A.; Thurston, G. M.; Blankshtein, D.; Benedek, G. B. *J. Phys. Chem.* **1990**, *94*, 2140.
- Foster, J. F.; Sterman, M. D. *J. Am. Chem. Soc.* **1956**, *78*, 3656.
- Steele, J. C. H.; Tanford, C.; Reynolds, J. A. *Methods Enzymol.* **1978**, *48*, 11.
- Liu, C.; Asherie, N.; Lomakin, A.; Pande, J.; Ogun, O.; Benedek, G. B. *Proc. Natl. Acad. Sci. U.S.A.* **1996**, *93*, 377.
- George, A.; Wilson, W. W. *Acta Crystallogr., Sect. D: Biol. Crystallogr.* **1994**, *50*, 361.

- (45) Kaye, W.; Havlik, A. *J. Appl. Opt.* **1973**, *12*, 541.
- (46) Tanford, C.; Swanson, S. A.; Shore, W. S. *J. Am. Chem. Soc.* **1955**, *77*, 6414.
- (47) Lebowitz, J. L.; Helfand, E.; Praestgaard, E. *J. Chem. Phys.* **1965**, *43*, 774.
- (48) Carnahan, N. F.; Starling, K. E. *J. Chem. Phys.* **1969**, *51*, 635.
- (49) Yethiraj, A.; Carol, K. H. *J. Chem. Phys.* **1991**, *95*, 8494.
- (50) Kulkarni, A. M.; Chatterjee, A. P.; Schweizer, K. S.; Zukoski, C. F. *J. Chem. Phys.* **2000**, *113*, 9863.
- (51) Tuinier, R.; Vliegthart, G. A.; Lekkerkerker, H. N. W. *J. Chem. Phys.* **2000**, *105*, 10768.
- (52) Eisenriegler, E.; Hanke, A.; Dietrich, S. *Phys. Rev. E* **1996**, *54*, 1134.
- (53) Reichl, L. E. *A Modern Course in Statistical Physics*; University of Texas Press: Austin, TX, 1980.
- (54) da Silva, L. H. M.; Coimbra, J. S. R.; de A. Meirelles, A. J. *J. Chem. Eng. Data* **1997**, *42*, 398.